Atmospheric Research 169 (2016) 24–31

Contents lists available at ScienceDirect

Atmospheric Research

journal homepage: www.elsevier.com/locate/atmos

Prediction of convective events using multi-frequency radiometric observations at Kolkata

Rohit Chakraborty, Saurabh Das, Animesh Maitra *

S. K. Mitra Centre for Research in Space Environment, Institute of Radio Physics and Electronics, University of Calcutta, Kolkata, India

ARTICLE INFO

Article history:
Received 21 April 2015
Received in revised form 22 September 2015
Accepted 25 September 2015
Available online 3 October 2015

Keywords:
Radiometer
Radiosonde
Nowcasting
Brightness temperature
Instability index
Convective rain

ABSTRACT

In the present study, the effectiveness of nowcasting convective activities using a microwave radiometer has been examined for Kolkata (22.65° N, 88.45° E), a tropical location. It has been found that the standard deviation of brightness temperature (BT) at 22 GHz and instability indices like Lifting Index (LI), K Index (KI) and Humidity Index (HI) has shown definite changes before convective events. It is also seen that combination of standard deviation of BT at 22 GHz and LI can be most effective in predicting convection. A nowcasting algorithm is prepared using 18 isolated convective events of 2011 and in all cases, a marked variation of these parameters has been seen an hour before the event. Accordingly, a prediction model is developed and tested on convective events of 2012 and 2013. It is seen that the model gives reasonable success in predicting convective rain about 7075 min in advance with a prediction efficiency of 80%.

1. Introduction

In the east and the north-eastern parts of the Indian subcontinent, intense convective activities are a very common feature. These types of activities occur during the pre monsoon period of March–May and are associated with severe lightning, heavy precipitation, hail and wind gusts. These activities also induce several adverse effects on various fields of life, such as agriculture and aviation. For this reason, prediction of such events has a very important implication on society.

In the past, short term prediction of convective activities is usually done using reflectivity echoes of impending storms using space borne and weather radars (Browning, 1982; Cluckie and Collier, 1991; Mecklenburg et al., 2000; Wang et al., 2009). However, there has not been much success in this regards because the less time span and localized nature of these activities make it difficult to predict them much in advance. Hermida et al. (2013) has studied the spatial variation and related climatological implications of hail storms which are accompanied with convective precipitation using a widely distributed network of 443 hailpads (ANELFA) covering various regions of France.

Knowledge based systems including radar, satellite, boundary layer profiler; lightning detector and upper air soundings are also being used for nowcasting intense convective activities. According to Kobler and Tafferner (2009) three parameters are important to understand the development of convection, namely, moisture, convective instability and lifting mechanism. Atmospheric temperature and humidity profiles and instability indices derived from atmospheric soundings like radiosondes can be very useful in nowcasting rain and thunderstorms (McCann, 1994; Geerts, 2001; Manzato, 2003; Midya et al., 2011; Midya and Saha, 2011; Saha et al., 2012; Chakraborty et al., 2015). However, radiosonde measurements suffer from poor temporal resolution. A microwave radiometer can generate humidity and temperature profiles of the atmosphere up to 10 km with high temporal resolution of 5 min and hence solves the problem faced by radiosondes. According to Chan and Lee (2011), alerting of wind shear can be done either by monitoring the stability of the boundary layer or by the standard deviations in the brightness temperature (BT) obtained from the microwave radiometer during both clear and cloudy skies at near elevation. The atmospheric water vapor and brightness temperatures around the water vapor absorption line measured by radiometer are used for such purposes (Won et al., 2009). The use of BT of oxygen absorption line along with water vapor can also predict rain with high accuracies (Chakraborty et al., 2014). In case of radiometric weather forecasting, two types of parameters are widely used — (1) utilization of level 0 products such as brightness temperatures and (2) parameters derived from BT measurements like Integrated Water Vapor (IWV), Liquid Water Content (LWC), Cloud Base Height (CBH) and instability indices (Koffi et al. 2007; Won

* Corresponding author at: Institute of Radio Physics and Electronics and Director, S. K. Mitra Centre for Research in Space Environment, University of Calcutta, 92, Acharya Prafulla Chandra Road, Kolkata-700009, India. Tel.: +91 33 2350 9116x28; fax: +91 33 2351 5828.
E-mail addresses: rohitc744@gmail.com (R. Chakraborty), das.saurabh01@gmail.com (S. Das), animesh.maitra@gmail.com, am.rpe@caluniv.ac.in (A. Maitra).

http://dx.doi.org/10.1016/j.atmosres.2015.09.024
0169-8095/

et al., 2009). These types of measurements are reported from different temperate regions; however, limited performance assessment of such techniques is available for tropical regions (Wilson et al., 1998). Won et al. (2009) obtained that an increase of Brightness Temperature (BT) is observed in water vapor channels (22–30 GHz) at about two hours (2 h) before rain. Güldner and Spänkuch (1999) have also obtained similar observations for an increase in the LWC and Precipitable Water Vapor (PWV) at about two hours (2 h) before rain. According to Chan (2009), the average values of K-index obtained from temperature and humidity profiles have a reasonable correlation with the tropospheric instability indicated by the number of lightning flashes within regions located about 10–40 km from the radiometer. Clifford et al. (2009) and Won et al. (2009) have studied the atmospheric conditions at boundary layer using radar, lidar, wind profiler and Radiometer. Many attempts have been made to predict convective activities using instability indices from atmospheric profilers (Faubush et al., 1951; Madhulatha et al., 2013; Showalter, 1953; Galway, 1956; Darkow, 1968; Chowdhury and Karmakar, 1986; Saha et al., 2014, 2015).

In the last few years, many attempts have been made to predict precipitation related activities. Dotzek and Forster (2011) had employed Cb-TRAM prediction algorithm with ESWD dataset for six severe weather days in Europe from 2007 to 2008 to detect storms in advance. The maximum prediction efficiency obtained for 30–60 min forecast was around 58%. Kohn et al. (2011) employed WDSS-II algorithm to nowcast thunderstorms using one year lightning data over the Mediterranean region. The technique was successful in predicting thousands of thunderstorms about 30 min in advance with a minimal False Alarm Rate (FAR) of 0.03 but with a very low Probability of Detection (POD) of 0.46. Dvorak et al. (2012) had devised a technique to detect precipitation and cloudiness using brightness temperature observations at 10 GHz from a microwave radiometer with a prediction efficiency of 80% and false alarm rate of around 15%. Later, Merino et al. (2014) developed a technique to identify hailstorms using MSG data obtained from the MEV valley in Spain from 2006 to 2010. The obtained technique called HDT employs two detection algorithms, namely convective mask and hail mask algorithms to detect hailstorms. This technique has provided an accuracy of 76.9% with a false alarm rate of 16.7%. As an extension of the previous work, Gascón et al. (2015) has designed another technique using forward stepwise regression algorithms on five major instability parameters. This system has a high POD of 0.94 but the FAR obtained was 0.22 which is quite high. However, it may be noted that most of the above said techniques have provided prediction efficiency less than 80% or a false alarm rate greater than 20%.

Recently, Chakraborty et al. (2014) had made an attempt to predict convective heavy rain using the fluctuations in BT of 22 and 58 GHz. A high prediction efficiency of 90% was obtained; however, the obtained lead time was low. This work is an improvement to the previous attempt where instability indices have been used along with the previously used BT at 22 GHz to predict convective rain in terms of increasing convective strength marked by high values of Convective Available Potential Energy (CAPE). The present technique also provides a better understanding of the changing atmospheric conditions before convective events. The reason for this is that convective activities are generally associated with unstable lapse rates and high moisture contents at three important pressure levels of the lower atmosphere, namely, 850 mbar, 700 mbar and 500 mbar pressures. BT at 58 GHz could manifest a decrease in ambient temperatures, but only in lower heights (generally < 2 km). In light of the above, it is expected that this technique might detect convective growth in a better way compared to the previous model.

2. Instrument description and data

A multi frequency profiler radiometer (RPG-HATPRO) situated on the roof top of the Institute of Radio Physics and Electronics, University of Calcutta (about 10 m above the ground level), has been used for the study. It consists of two receiving units, a data acquisition system, rain sensor, GPS clock, and ground meteorological sensor (Rose and Czekala, 2009). This instrument measures brightness temperatures with a high temporal resolution of 3 s in a range of 0–800 K and provides an accuracy of 0.5 K at 14 frequency channels in two separate bands. The first frequency band (22–31.4 GHz) is sensitive to water vapor and hence is utilized for humidity profiling. The second frequency band (51.26–58 GHz), is sensitive to oxygen absorption and hence is utilized to obtain the temperature profiles. These brightness temperature datasets are then smoothed for a time window of 3 min (60 samples) to remove any unwanted fluctuations. Quadratic regression techniques are utilized to transform brightness temperature values into several atmospheric parameters like profiles of temperature and humidity, IWV and a series of instability indices, namely Lifted Index (LI), K-Index (KI), Totals Total Index (TTI) and Showalter Index (SI).

For the present study, brightness temperature and instability index observations from Radiometer for 18 convective events during 12 convective days and 58 non-convective days of March–May 2011 have been used. For validation of the prediction technique, radiometric data of 40 convective events during 28 days of March–May 2012 and 2013 has been utilized. A set of four parameters has been used to develop an algorithm to nowcast convective activities. They are LI, KI, BT standard deviation and HI.

The brightness temperature at 22 GHz indicates the amount of vapor in the atmosphere. Strong convective activities usually require bulk concentration of atmospheric water vapor. So these changes in the atmospheric vapor density prior to the event can be clearly indicated by large values of BT at 22 GHz. However, BT values show strong seasonal and diurnal variation; hence a change in this parameter related to convection can be indicated by an increase in its standard deviation value. For this reason, a 30 minute standard deviation of BT at 22 GHz has been included in the analysis instead of its absolute value.

The Lifting Index (LI) denotes the stability of air parcels. When an air parcel is lifted adiabatically to a height of 500 bar pressure then the parcel temperature and the environmental temperatures at that height are compared. Negative or near negative value of LI reflects condensation of saturated vapor parcel to liquid indicating instability and severe weather conditions.

The K-Index measures the thunderstorm potential in terms of the vertical temperature lapse rate between 850 and 500 mbar pressure levels, the moisture content at 850 mbar pressure and the depth of the moist layer at 700 mbar pressure level (George, 1960). KI values close to 30 K indicate severe weather conditions (Haklander and van Delden, 2003).

The Humidity index shows the difference of the dew point and environment temperature at various pressure levels of the atmosphere. These temperature differences at each level denote the degree of saturation of vapor and the extent of condensation at those layers. Lower values (HI < 30 K) indicate instability at all three pressure levels of the lower atmosphere (850, 700 and 500 mbar pressure levels) thereby indicating severe weather conditions (Litynska et al., 1976).

In this study, various instability indices have been used to predict convective activities. However, the strength of these activities can best be quantified by their convective available potential energy (CAPE). According to Emmanuel (1994), CAPE indicates the buoyant energy available to accelerate an air parcel vertically. It can be calculated using the summation of positive buoyant energy from the level of free convection (height where the parcel temperature > environment temperature) to the Equilibrium Level (height where parcel temperature = environment temperature). Higher CAPE provides more energy for convective growth; hence CAPE should be high in convective conditions and less in normal conditions. Rasmussen and Wilhelmson (1983) have mentioned that values of CAPE > 1500 J kg^{-1} are suitable for super cell formation. Hence the occurrence of CAPE values greater than 1500 J kg^{-1} is considered to be an indicator of the impending convective rain.

It should be noted that out of these 5 parameters, only the BT at 22 GHz is obtained directly from a microwave radiometer. KI and LI and CAPE are obtained by applying the quadratic regression analysis of the brightness temperature data are obtained and are time averaged to give values after every three minutes. However, the value of HI has been calculated from the relative humidity and temperature profiles of radiometer observations.

To have a quality check of the data, the brightness temperatures and retrieved instability indices and CAPE obtained from radiometer are compared with co-located radiosonde observations (taken at 00:00 h from IMD Kolkata, located < 10 km from the research facility) for 80 days during March–May 2011. Five parameters from both the instruments have been compared. They are the ground temperature and relative humidity, PWV, KI and CAPE. The comparison between the parameters obtained from both the instruments is shown in Fig. 1.

From Fig. 1 it can be inferred that the radiometric results have a good correlation with radiosonde measurements. Reasonably high correlation coefficients have been obtained between the two instruments in all the five parameters. It has been found that there are some small errors in the relative humidity profiles. These errors are due to wet bias errors which are generally prevalent in the height range of 1–6 km. Many researchers have reported the existence of such type of biases (Chan, 2009; Xu et al., 2014). However, it has been found that the biases given by the radiometer are comparable to other studies as reported earlier (Chan, 2009; Chakraborty et al., 2014; Xu et al., 2014). Sánchez et al. (2013) had compared vertical profiles of temperature and water vapor from multi channel microwave radiometer observations with thousands of radiosonde profiles and obtained an error bias of 0.2–1.2 K in temperature and 0.05– 0.5 g m^{-3} in water vapor profiles.

In addition to all this, an impact type disdrometer (RD-80, Waldgovel type) has also been used for rain rate measurements. The rain events having a minimum duration of 10 min with a maximum instantaneous rain rate magnitude greater than 20 mm h^{-1} have been considered for the study. A set of 18 convective events and 58 non convective events of 2011 have been utilized for testing the proposed model, while 40 convective events of 2012 have been used for validation purposes. The decision of whether an event is convective or not, has been taken based on the criterion of the absence of bright band structures in the radar reflectivity profiles observed with a collocated MRR at our research facility as already discussed in previous studies (Das et al., 2011; Maitra et al., 2014; Sarkar et al., 2015).

3. Methodology

During convection, the temperature of the lower atmosphere increases resulting in low pressure and convective wind currents. These convective currents result in updraft of moisture laden winds causing cloud formation and in an increase of humidity. Consequently, the clouds above the region starts getting saturated, which finally results in a condensation of vapor to liquid with an emission of latent heat. In this process, the temperature balance in all the layers of lower atmosphere gets disturbed leading to thermodynamic instability. During the same time, hot air ascending from the surface goes up, gets cooled down and then descends to the surface resulting in intense downdrafts (Wakimoto, 1982). Now this process results in an increase in moisture in the lower levels and an unstable lapse rate between 850 and 500 mbar pressure levels. The increase in moisture can always be manifested by a significant increment in 22 GHz brightness temperatures owing to the high absorption of water vapor at 22–31 GHz. The instability index parameters also show a definite change before the events.

In previous studies, there have been attempts to predict intense convective rain using brightness temperatures at 22 and 58 GHz. However, the technique did not turn out to be effective as the obtained lead time was very small. From previous studies, it can be inferred that convective life cycle has three definite steps, namely; growth, maturity and dissipation. It is also known that rain occurs during the dissipation stage, so their genesis can be conveniently manifested by monitoring the growth of such activities.

In this study it has been attempted to indicate convective growth using the instability indices instead of using the brightness temperature at 58 GHz. As a convective system develops, hot air goes up and disturbs the heat balance of the atmosphere resulting in a change in instability which could be indicated by a change in the instability indices much before rain. However, when this hot air goes up, it cools to form a cloud which matures to form rain drops that cool down the surrounding air causing cold downdrafts before rain reaches the ground level. This phenomenon causes a cooling effect which can be manifested by a decrease in BT at 58 GHz. Hence, the use of instability indices in the model might

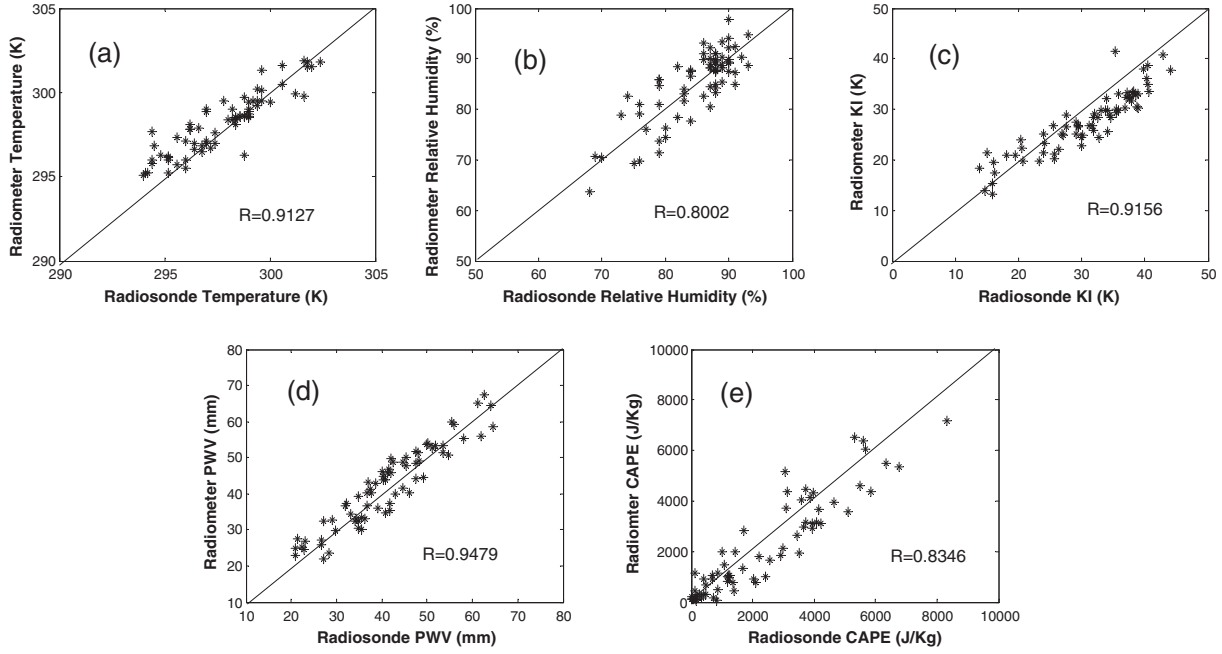

Fig. 1. Correlation analysis between Radiometer and Radiosonde (a) temperature (b) relative humidity, (c) PWV, (d) KI and (e) CAPE.

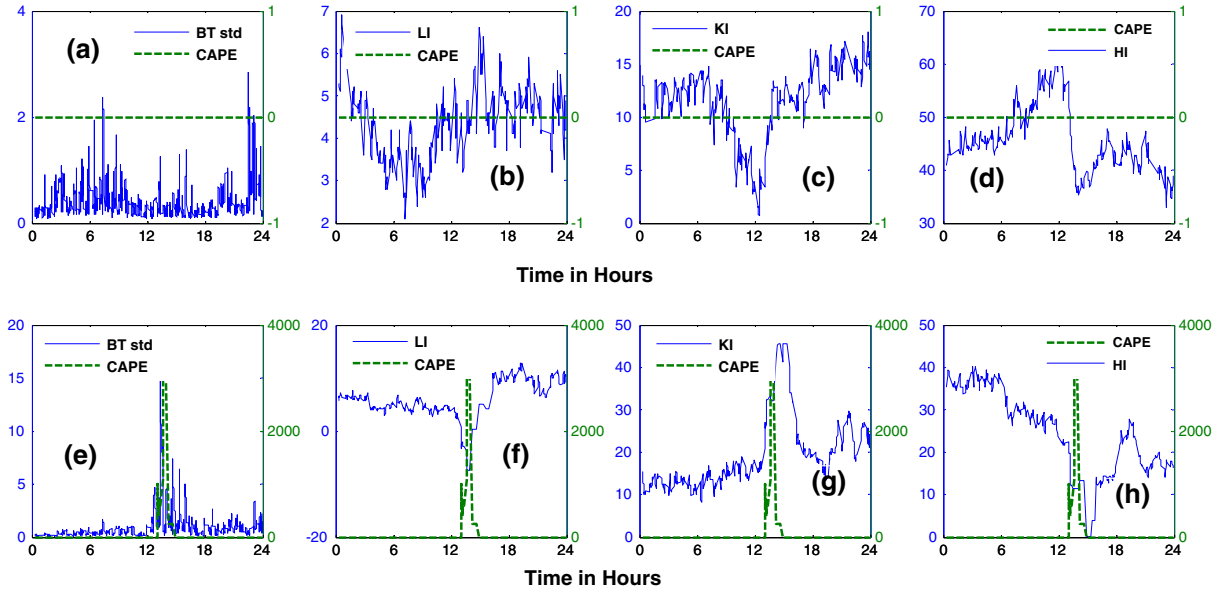

Fig. 2. Hourly variation of parameters with respect to CAPE during Case 1, a non-convective day (April 2, 2011) (a) standard deviation of BT at 22 GHz (K), (b) LI (K), (c) KI (K) and (d) HI (K) and Case 2, during a convective day (April 4, 2011), (e) standard deviation of BT at 22 GHz (K), (f) LI (K), (g) KI (K) and (h) HI (K). The parameters are indicated by solid blue line and while CAPE (J kg^{-1}) is indicated by a green dotted line.

improve the rain forecast lead time compared to the brightness temperatures at 58 GHz.

It has already been mentioned in the previous sections that high CAPE values have been used as an indicator of convection. As a result, 18 convective events, witnessing heavy rain (~20 mm h^{-1}) in the period of March–May 2011, are selected. The period of March–May is selected because this time of the year witnesses intense convective activities due to thunderstorms generated from westerly currents. Next, the frequency distribution of the time gap between the rain event start and high CAPE occurrences is seen and it is found that CAPE rises to about 1500 J kg^{-1} about 10 min before the start of rain.

Now, four parameters have been used to manifest convective growth marked by high CAPE (value > 1500 J kg^{-1}), namely, the standard deviation of 22 GHz BT, LI, KI and HI. In order to indicate the difference between a non-convective and a convective day, these four parameters are observed in April 4, 2011 a convective day, and April 2, 2011 which is a non convective day. The results are shown in Fig. 2.

From Fig. 2, the differences can be seen between the parameters observed in April 2, 2011 and April 4, 2011 (hereafter named as Case 1 and Case 2 respectively). LI in Case 1 remains within the range 3–7 K while in Case 2, it becomes negative just before the event. For 22 GHz BT standard deviation in Case 1 the range is 0–2.5 K while in Case 2 it increases

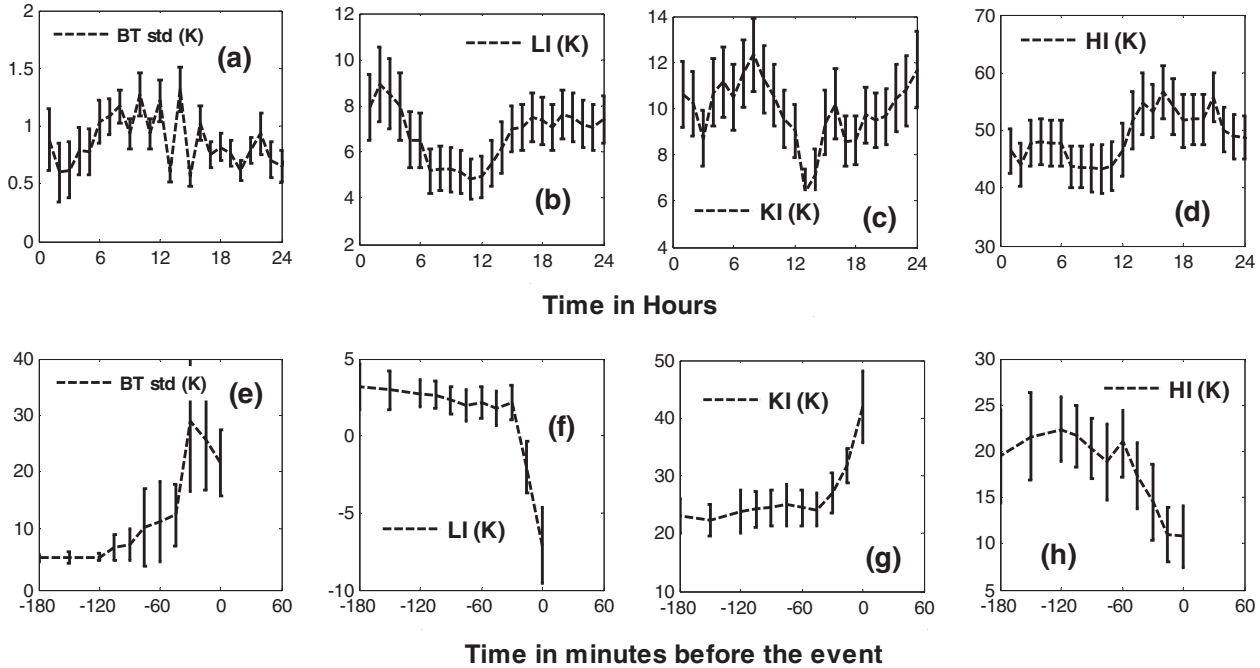

Fig. 3. Average variation of parameters for non-convective days: (a) standard deviation of BT at 22 GHz, (b) LI, (c) KI and (d) HI and for convective days: (e) standard deviation of BT at 22 GHz, (f) LI, (g) KI and (h) HI.

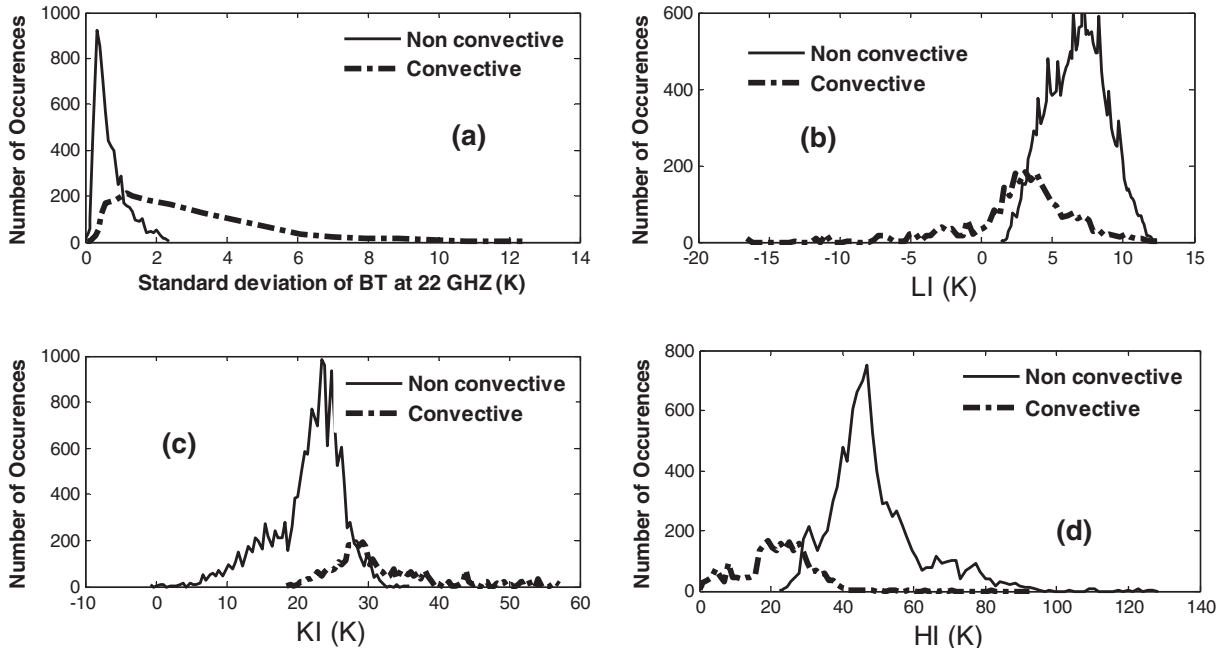

Fig. 4. Frequency distribution of parameters for non-convective days and for convective days (a) standard deviation of BT at 22 GHz, (b) LI, (c) KI and (d) HI.

to a value above 4 K shortly before the event. For KI the range is 0–15 K in Case 1 but the value increases and reaches up to 30 K before the event. In case of HI, the parameter range is above 40 K in Case 1 while in Case 2, value decreases to about 15 before the event.

Now, it becomes important to verify whether these parameters show a change due to some definite atmospheric processes or due to some random phenomenon. For this reason, a set of 58 non-convective days of 2011 is selected and the hourly diurnal variation of these parameters has been studied in Fig. 3. The average variation of these parameters has also been shown for the 18 convective test events of 2011 to visualize the difference in these parameters in the presence of convection. These parameters have been recorded from up to three hours before the convective event (marked by high CAPE). All these four parameters have been time averaged for an interval of 30 min in case of non convective days. However, for convective days, the parameters were time averaged on an interval of 30 min from 3 to 2 h before the event and then at an interval of 15 min from 2 h before the event till the start of the event. The standard deviations have also been shown in error bars to signify the maximum variation of these parameters. From the figure, it can be seen that LI is generally in the range of 3–10 K during non convective days, but before the event it falls down to 0 K. The standard deviation of 22 GHz remains in the range 0–2 K in non convective days while in convective cases, it starts increasing before the event. KI generally stays in the range of 0–30 K but it starts rising to 50 K before the event. Again, HI remains normally in the range 35–70 K but it starts decreasing up to 10 K before the event. It is also seen from the figure

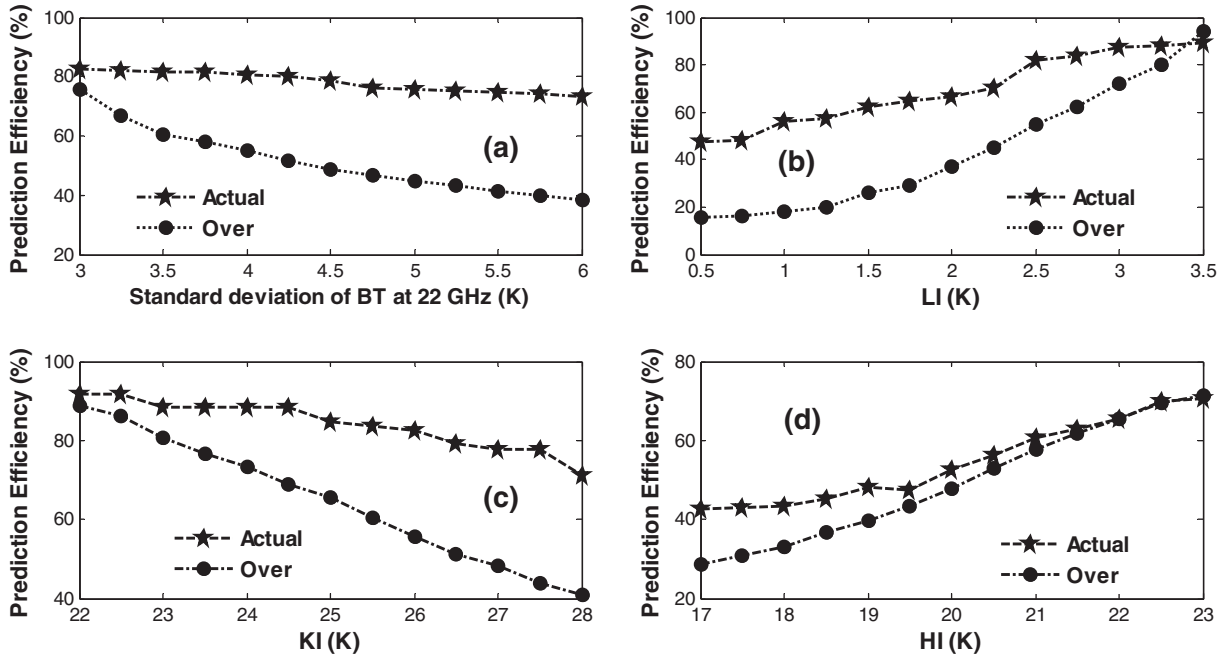

Fig. 5. Variation of prediction efficiency with individual parameters (a) LI, (b) standard deviation of BT at 22 GHz, (c) KI and (d) HI.

Table 1
Variation of prediction efficiencies for different combinations of model parameters.

Serial no.	Parameters used	Actual efficiency (%)	False prediction (%)
1	LI & KI	80.33	52.77
2	BT & KI	70.78	34.67
3	***LI & BT***	***79.12***	***18.35***
4	LI & HI	66.76	45.94
5	BT & HI	69.54	31.88
6	KI & HI	64.7	54.85
7	BT,HI & LI	70.34	17.67
8	HI,KI & BT	70.45	23.88
9	KI,BT & LI	76.54	19.2
10	KI,HI & LI	72.37	26.68
11	KI,LI,HI & BT	72.73	16.17

that in case of non convective days, a strong diurnal variation occurs. However, the magnitudes obtained by the four parameters before convection is much distinct from the overall range of these parameters in case of non convective days.

Now, it is essential to find the quantitative difference between the magnitude of all these four parameters for a non convective day and a convective day. For this reason, the magnitudes of all these four parameters have been recorded for 12 convective days and 58 non convective days of 2011 and the frequency distribution of these parameters are observed as shown in Fig. 4.

From Fig. 4 it can be seen that there is a definite difference between the ranges of these parameters during convective and non convective days. For example, during non convective days, LI generally varies in the range is 5–15 K while in convective days it is −5 to 10 K which indicates the occurrence of atmospheric instability. For standard deviation of the brightness temperature at 22 GHz, the range is 0–2.5 K for non convective days while for convective cases it is in the range 0–10 K again indicating more variation in vapor density before convective events. For KI during non convective days the value ranges from −20 to 20 K while for convective days it is 0–50 K indicating a higher potential to create storms. Again, HI showed a range of 30–80 K for non convective and 0–40 K for convective days respectively indicating the development of saturated atmosphere before convective activities. So, from this Figure it can be said that all these four parameters show definite change before convection, indicating their usefulness in nowcasting convective events.

4. Prediction model for convection events

A model has been developed which checks the magnitude of these parameters with a sliding window of 30 min and generates an alarm for the occurrence of convective events whenever any of these parameters crosses a definite threshold. The threshold value for each parameter has been obtained which is as follows. First, the ranges for which these parameters are to be checked have been obtained from the frequency distribution analysis as shown in Fig. 4. It is found that for LI the range is 0–3 K, for the standard deviation of BT at 22 GHz it is above 4 K, for KI it is above 23 K and for HI it is below 30 K. Out of these ranges of values obtained from the frequency distribution, a suitable threshold value can selected on basis of two model performance parameters. First one is the actual prediction efficiency while the second one is the over prediction rate. Whenever the model generates an alarm and convection occurs within the next one and half hour, then it is considered as a success. Number of events successfully predicted divided by the total number of convective events give the actual prediction efficiency. However, when an alarm is generated, but convective activity has not occurred within the next 90 min then it is a false prediction. The number of false predictions divided by the number of non convective conditions gives the over prediction or false alarm rates. Now based on these two performance parameters, the prediction model is run for each value in the prescribed range. Out of these parameter values only one value is selected to be the threshold for which the prediction efficiency is maximum (at least greater than 70%) and the over prediction is the least. The prediction efficiencies and over prediction rates have been obtained and shown for all the four parameters individually in Fig. 5. As seen from this figure, the optimum value for LI, Standard deviation, KI and HI are taken to be 2.6 K, 4.5 K, 27 K and 22.5 K respectively.

From Fig. 5, it can be inferred that for each of these individual parameters, an optimum prediction efficiency of ~80% has been reached, but the over prediction rate is still very high (~35%). So, to reduce the over prediction rate, a systematic grouping of these four parameters is considered to form various parameter combinations. The criterion for selecting a combination to be optimized is the highest actual prediction and lowest over prediction rate obtained from it. A list of the resulting prediction efficiencies is shown in Table 1. From the table, it is seen that a combination of LI and standard deviation of BT of 22 GHz can bring optimum prediction efficiency. To find out whether any improvement in the system performance is achieved using more than two variables, the same analysis is done for all combinations of three elements together as shown in the Table 1. As seen from the table, there are no significant improvements in the performance limits. The reason for this is, though the over prediction rate has been reduced considerably after the implementation of these parameters; the actual prediction efficiency has also gone below 75% which might not be favorable for the nowcasting technique. The same results are also found when all parameters are used in the algorithm. Hence, finally a combination of BT standard deviation and LI is taken.

From Fig. 6(a) it can be seen that when the values of LI and Standard deviation of BT at 22 GHz are around 2.6 K and 4.5 K respectively, an

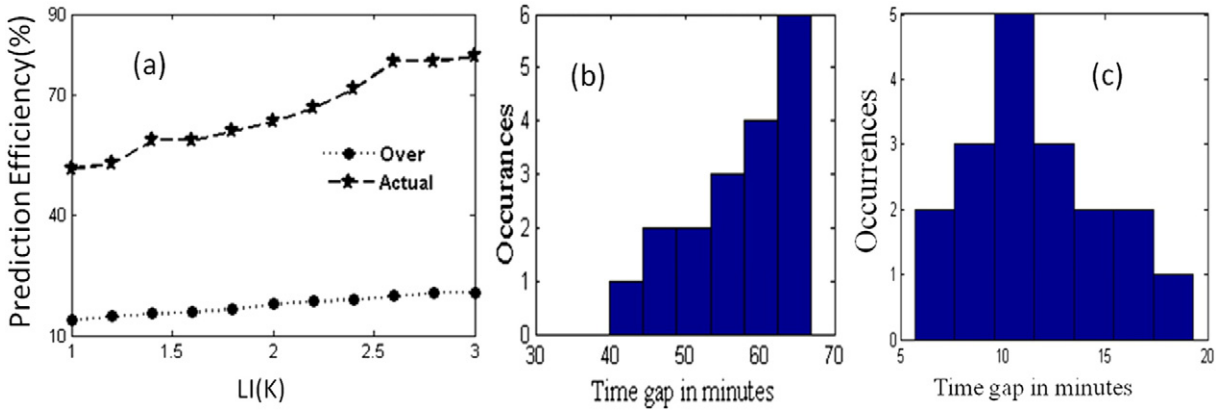

Fig. 6. (a) Variation of Prediction Efficiency with parameters LI with standard deviation of BT of 22 GHz fixed at 4.5 (optimum), (b) frequency distribution of time gaps between CAPE and alarm generation, (c) frequency distribution of time gap between CAPE and rain occurrence.

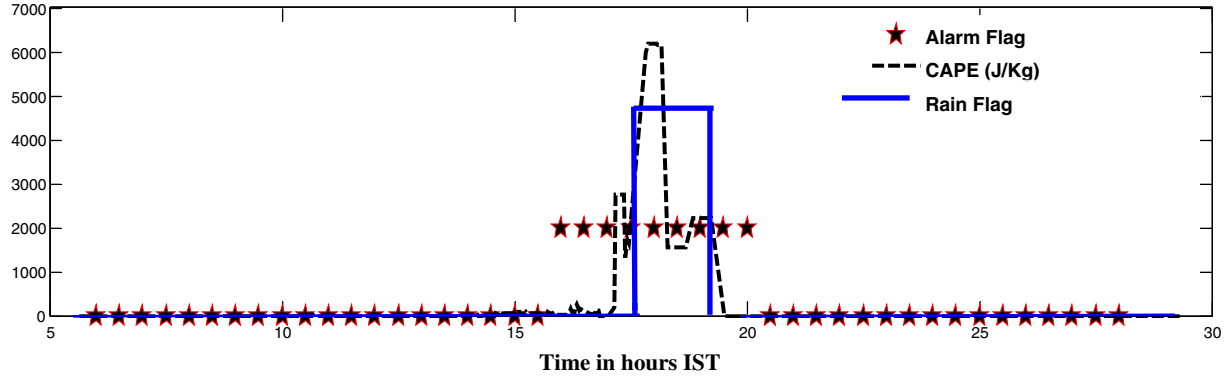

Fig. 7. Result of the simulated model for a convective event May 20, 2012.

optimum actual prediction efficiency of ~ 80% is obtained with an over prediction rate of ~18%. Next, the lead time, which refers to the time gap between the generation of alarms and the occurrence of high CAPE values (CAPE > 1500 J kg^{-1}) is recorded. The frequency distribution of these time gaps indicates that the alarm mostly gets activated about 65 − 70 min before high CAPE occurrence as shown in Fig. 6(b). It can also be observed from the figure that the model generates alarm successfully at around 55 min before the start of convective event for 70% cases. The mean of the warning time is also found to be around 60 min. At the same time, the frequency distribution of the time gap between high CAPE and the start of rain event has also been recorded as shown in Fig. 6(c). From the figure, it can be seen that in most of the cases, CAPE goes high about 11 min before start of rain. Hence it follows that this technique can manifest rain occurrence about 60 + 11–70 min before the event.

5. Validation

The prediction technique has now been tested in a set of 40 independent convective events of 2012 and 2013. An actual prediction efficiency of 78% and an over prediction rate of around 16% has been obtained. The time gap between an alarm generation and high CAPE and also the time gap between CAPE and rain occurrence are recorded for each event. It is seen that the alarm is mostly generated around 75 min before the rain event. Fig. 7 shows a typical convective event on 20 May 2012 for which an alarm is generated about 90 min before the start of rain.

6. Conclusions

The primary objective of the present study is to utilize a microwave radiometer in predicting severe convective weather over Kolkata. For this purpose, radiometric data of premonsoon 2011 have been utilized. Four parameters like KI, LI, HI and the standard deviation of BT at 22 GHz obtained from radiometer have been used in this study. It is found that all these four parameters show a definite variation before the event which is not present for non convective days. A nowcasting model has been developed using various combinations of instability parameters to generate an alarm in every 30 min in case of convective events. It is seen that that a combination of LI and standard deviation of BT at 22 GHz can be most effective to nowcast convective activities with prediction efficiencies of about 80% and an over prediction rate of 18%. The proposed model performed reasonably well when it is tested for a number of convective events of 2012 and 2013 with an effective lead time of about 70–75 min before rain. In a previous study, it was shown that convective rain has been predicted with 90% prediction accuracy and a lead time of 25 min. However, this technique provides an accuracy of 80%, but here the alarm is generated about 75 min before rain. Nevertheless, this model provides a significant improvement over the previous technique. In this technique, the lead time has increased from about 25 min in the previous case to about 75 min, which makes it more suitable to predict convective events well in advance. Secondly, this technique helps to give a better understanding of the pre-convective atmosphere as it tracks the convective growth in terms of changing atmospheric instability. Apart from this, the prediction efficiency obtained from this technique has been almost comparable to those obtained from other studies as already mentioned in the introduction section, indicating the model's suitability in predicting weather extremes in a less involved way compared to RADAR and satellite measurements. The present technique can therefore serve as a useful tool to nowcast convective events.

Acknowledgment

The financial support provided by ISRO under the projects (1) “Space Science Promotion Scheme” with grant no. E 33013/3/2009-V and (2) “Ku/Ka Band channel modeling for SATCOM links over Indian Region” with grant no. ISRO/RES/4/614/2014-15 dated 02.06.2014, is thankfully acknowledged.

References

Browning, A.K., 1982. A Very Short Range Forecasting of Precipitation by the Objective Extrapolation of Radar and Satellite Data in Nowcasting. Academic Press, U.S.A, p. 177.
Chakraborty, R., Das, S., Jana, S., Maitra, A., 2014. Nowcasting of rain events using multi-frequency radiometric observations. J. Hydrol. 513, 467–474.
Chakraborty, S., Saha, U., Maitra, A., 2015. Relationship of convective precipitation with atmospheric heat flux — a Regression approach over an Indian tropical location. Atmos. Res. 161–162, 116–124. http://dx.doi.org/10.1016/j.atmosres.2015.04.008.
Chan, P.W., 2009. Performance and application of a multi-wavelength, ground based microwave radiometer in intense convective weather. Meteorol. Z. 18 (3), 253–265.
Chan, P.W., Lee, Y.F., 2011. Application of ground based multi-channel microwave radiometer to the alerting low level wind shear. Meteorol. Z. 20 (4), 423–429.
Chowdhury, M.H.K., Karmakar, S., 1986. Premonsoon nor'westers in Bangladesh with case studies. Proc. Seminar on Local Severe StormsBangladesh Meteorological Department, Dhaka, pp. 147–166.
Clifford, S.F., Kaimal, J.C., Lataitis, R.J., Strauch, R.G., 2009. Ground based remote profiling in atmospheric studies, an overview, proceedings. IEEE 82, 313–355.
Cluckie, I.D., Collier, C.G., 1991. The combined use of weather radar and mesoscale numerical model data for short-period rainfall forecasting. Hydrological Applications of Weather Radar. Academic Press, New York, pp. 331–348.
Darkow, G.L., 1968. The total energy environment of severe storms. J. Appl. Meteorol. Climatol. 7 (2), 199–205.
Das, S., Talukdar, S., Bhattacharya, A., Adhikari, A., Maitra, A., 2011. Vertical profile of Z-R relationship and its seasonal variation at a tropical location. IEEE Proceedings of Applied Electromagnetics Conference (AEMC) http://dx.doi.org/10.1109/AEMC.2011.6256915.
Dotzek, N., Forster, C., 2011. Quantitative comparison of METEOSAT thunderstorm detection and nowcasting with in situ reports in the European Severe Weather Database. Atmos. Res. 100 (4), 511–522.
Dvorak, P., Mazanek, M., Zvanovec, S., 2012. Short-term prediction and detection of dynamic atmospheric phenomena by microwave radiometer. Radioengineering 21 (4), 1060–1066.
Emmanuel, K.A., 1994. Atmospheric Convection. Oxford University Press (580 pp).
Faubush, E.J., Miller, R.C., Starrett, L.G., 1951. An empirical method for forecasting tornado development. Bull. Am. Meteorol. Soc. 32, 19.

Galway, J.G., 1956. The lifted index as a predictor of latent instability. Bull. Am. Meteorol. Soc. 37, 528–529.
Gascón, E., Merino, A., Sánchez, J.L., Fernandez, S.-G., Edurado, G.-O., López, L., Hermida, L., 2015. Spatial distribution of thermodynamic conditions of severe storms in south-western Europe. Atmos. Res. 164–165, 194–209.
Geerts, B., 2001. Estimating downburst related maximum surface wind speeds by means of proximity soundings in New South Wales, Australia. Weather Forecast. 16, 261–269.
George, J.J., 1960. Weather Forecasting for Aeronautics. Academic Press, New York, pp. 407–415.
Güldner, J., Spänkuch, D., 1999. Result of year round remotely sensed integrated water vapour by ground based microwave radiometry. J. Appl. Meteorol. Climatol. 38, 981–988.
Haklander, A., van Delden, A.J., 2003. Thunderstorm predictor and their forecast skill for the Netherlands. Atmos. Res. 67–68, 273–299.
Hermida, L., Sanchez, J.L., Lopez, L., Berthet, C., Dessens, J., Eduardo, G.-O., Merino, A., 2013. Climatic trends in hail precipitation in France: spatial, altitudinal and temporal variability. Sci. World J. 2013, 494971 (1–10).
Kobler, K., Tafferner, A., 2009. Tracking and nowcasting of convective cells using remote sensing data from radar and satellite. Meteorol. Z. 1, 75–84.
Koffi, E.N., Schneebeli, M., Brocard, E., Mätzler, C., 2007. The Use of Radiometer Derived Convective Indices in Thunderstorm Nowcasting, Mätzler Research Report Nr. 2007-02-MW. Bern University.
Kohn, M., Galanti, E., Price, C., Lagouvardos, K., Kotroni, Kostas, V., 2011. Nowcasting thunderstorms in the Mediterranean region using lightning data. 5th European Conference on Severe Storms. 100, pp. 489–502. http://dx.doi.org/10.1016/j.atmosres.2010.08.010 (4).
Litynska, Z., Parfiniewicz, J., Pinkowski, H., 1976. The prediction of air mass thunderstorms and hail. World Meteor. Org. Bull. 450, 128–130.
Madhulatha, A., Rajeevan, M., Venkat Ratnam, M., Bahte, J., Naidu, C.V., 2013. Nowcasting severe convective activity over southeast India using ground based microwave radiometer observations. J. Geophys. Res.: Atmos. 118, 1–13.
Maitra, A., Jana, S., Chakraborty, R., Majumder, S., 2014. Multi-technique observations of convective rain events at a tropical location. Proceedings of General Assembly and Scientific Symposium (URSI GASS), 2014 XXXIth URSI http://dx.doi.org/10.1109/URSIGASS.2014.6929640.
Manzato, A., 2003. A climatology of instability indices derived from Friuli Venezeilia Giulia soundings using three different methods. Atmos. Res. 67–68, 417–454.
McCann, D.W., 1994. WINDEX — a new index for forecasting microburst potential. Weather Forecast. 9, 532–541.
Mecklenburg, S., Joss, J., Schmid, W., 2000. Improving the nowcasting of precipitation in an Alpine region with an enhanced radar echo tracking algorithm. J. Hydrol. 239, 46–68.
Merino, A., López, L., Sánchez, J.L., Edurado, G.-O., Cattani, E., Levizzani, V., 2014. Day-time identification of summer hailstorm cells from MSG data. Nat. Hazards Earth Syst. Sci. 14, 1013–1034.
Midya, S.K., Saha, U., 2011. Rates of change of total ozone column and surface relative humidity: seasonal variations over Dum Dum (22° 38′ N, 88° 26′ E). Int. J. Remote. Sens. 32 (22), 7891–7899. http://dx.doi.org/10.1080/01431161.2010.531789.
Midya, S.K., Sarkar, H., Saha, U., 2011. Sharp depletion of atmospheric refractive index associated with Nor'wester over Gangetic West Bengal: a possible method of forecasting Nor'wester. Meteorog. Atmos. Phys. 111, 149–152. http://dx.doi.org/10.1007/s00703-011-0122-3.
Rasmussen, R.M., Wilhelmson, R.B., 1983. Relationships between storm characteristics and 1200GMT hodographs, low-level shear and stability. Proceedings of the13th Conference on Severe Local Storms. American Meteorological Society, Tulsa, Okla, USA, pp. 55–58.
Rose, Th., Czekala, H., 2009. RPG-HATPRO Radiometer Operating Manual, Radiometer Physics GmbH, Version 7.99.
Saha, U., Midya, S.K., Sarkar, H., Das, G.K., 2012. Sharp depletion of absolute humidity associated with squall over Kolkata (22°34′N, 88°26′E): a possible method of forecasting squall. Pacific J. Sci. Technol. 13 (1), 683–688.
Saha, U., Maitra, A., Midya, S.K., Das, G.K., 2014. Association of thunderstorm frequency with rainfall occurrences over an Indian urban metropolis. Atmos. Res. 138, 240–252. http://dx.doi.org/10.1016/j.atmosres.2013.11.021.
Saha, U., Chakraborty, R., Maitra, A., 2015. Asymmetry in The Variability Of Pre-Monsoon Surface Wind — A Long-Term Study Over Coastal Boundaries Of The Indian Sub-Continent, Under Review In Atmos. Res.
Sánchez, J.L., Posada, R., Edurado, G.-O., López, L., Marcos, J.L., 2013. A method to improve the accuracy of continuous measuring of vertical profiles of temperature and water vapour density by means of a ground-based microwave radiometer. Atmos. Res. 122, 43–54.
Sarkar, T., Das, S., Maitra, A., 2015. Assessment of different raindrop size measuring techniques: inter-comparison of Doppler radar, impact and optical disdrometer. Atmos. Res. 160, 15–27.
Showalter, A.K., 1953. Stability index for forecasting thunderstorms. Bull. Am. Meteorol. Soc. 34, 250–252.
Wakimoto, R.M., 1982. The life cycle of thunderstorm gust fronts as viewed with Doppler radar and radiosonde data. Mon. Weather Rev. 110, 1060–1082.
Wang, P., Smeaton, A., Lao, S., O'Connor, E., Ling, Y., O'Connor, N., 2009. Short-Term Rainfall Nowcasting: Using Rainfall Radar Imaging, Eurographics, Ireland.
Wilson, J.W., Crook, A.N., Mueller, C.K., Sun, J., Dixon, M., 1998. Nowcasting thunderstorms: a status report. Bull. Am. Meteorol. Soc. 79, 2079–2099.
Won, H.Y., Kim, Y.H., Hee-Sang, 2009. Application of brightness temperature received from ground-based microwave radiometer to estimation of precipitation occurrences and rainfall intensity. Asia Pacific. J. Atmos. Sci. 45, 55–69.
Xu, G., Randolph, W., Zhang, W., Feng, G., Liao, K., Liu, Y., 2014. Effect of off-zenith observations on reducing the impact of precipitation on ground-based microwave radiometer measurement accuracy. Atmos. Res. 140–141, 85–94.